energies

MDPI

Article

Phase Equilibria of the CH_4-CO_2 Binary and the CH_4-CO_2-H_2O Ternary Mixtures in the Presence of a CO_2-Rich Liquid Phase

Ludovic Nicolas Legoix [1,2,*], Livio Ruffine [2,*], Jean-Pierre Donval [2] and Matthias Haeckel [1]

1 GEOMAR, Helmholtz Centre for Ocean Research Kiel, Wischhofstr. 1-3, D-24148 Kiel, Germany; mhaeckel@geomar.de

2 Institut Français de Recherche pour l'Exploitation de la Mer (IFREMER), Centre de Bretagne, Département Ressources physiques et Ecosystèmes de fond de Mer, Unité des Géosciences Marines, BP70, 29280 Plouzané, France; jean.pierre.donval@ifremer.fr

* Correspondence: llegoix@geomar.de (L.N.L.); livio.ruffine@ifremer.fr (L.R.)

Received: 20 September 2017; Accepted: 28 November 2017; Published: 2 December 2017

Abstract: The knowledge of the phase behavior of carbon dioxide (CO_2)-rich mixtures is a key factor to understand the chemistry and migration of natural volcanic CO_2 seeps in the marine environment, as well as to develop engineering processes for CO_2 sequestration coupled to methane (CH_4) production from gas hydrate deposits. In both cases, it is important to gain insights into the interactions of the CO_2-rich phase—liquid or gas—with the aqueous medium (H_2O) in the pore space below the seafloor or in the ocean. Thus, the CH_4-CO_2 binary and CH_4-CO_2-H_2O ternary mixtures were investigated at relevant pressure and temperature conditions. The solubility of CH_4 in liquid CO_2 (vapor-liquid equilibrium) was determined in laboratory experiments and then modelled with the Soave–Redlich–Kwong equation of state (EoS) consisting of an optimized binary interaction parameter $k_{ij(CH_4\text{-}CO_2)} = 1.32 \times 10^{-3} \times T - 0.251$ describing the non-ideality of the mixture. The hydrate-liquid-liquid equilibrium (HLLE) was measured in addition to the composition of the CO_2-rich fluid phase in the presence of H_2O. In contrast to the behavior in the presence of vapor, gas hydrates become more stable when increasing the CH_4 content, and the relative proportion of CH_4 to CO_2 decreases in the CO_2-rich phase after gas hydrate formation.

Keywords: gas hydrate; CH_4; CO_2-rich mixtures; phase equilibria; Soave–Redlich–Kwong (SRK) cubic equation of state (EoS)

1. Introduction

CO_2 is ubiquitous in geological systems, and is encountered in geofluids in multiple phases (e.g., Lewicki et al. [1], Boiron et al. [2]). Generally, it is either generated by the degradation of organic matter, decomposition of carbonate rock, or post-genetic mantle processes. However, the occurrence of a CO_2-rich gaseous, liquid, and gas hydrate phase is typically limited to volcanic systems [3–6], where it is often accompanied by admixtures of hydrocarbon gases such as CH_4. Reconstructing the migration pattern of such fluids from their source within the sedimentary column to their discharge and fate into the H_2O column requires a correct understanding of the involved thermodynamic phase equilibria. In addition, as society is increasingly concerned about mitigating CO_2 emissions into the atmosphere, understanding the phase behavior of CO_2-rich mixtures becomes more important for the design and conception of reliable carbon storage processes. Amongst the processes under investigation, the storage of CO_2 in solid gas hydrates by replacing the CH_4 from natural accumulations seems to be very promising, since it helps to meet the global energy demand, while reducing net global carbon emissions. CH_4 production from gas hydrates coupled to CO_2 sequestration has been investigated

intensively; e.g., with some laboratory-scale experiments [7–11], and in a field-scale production test [12]. The method involves multiple phase equilibria, where a liquid aqueous and a CO_2-rich phase coexist with vapor and solid gas hydrates, depending on the prevailing temperature and pressure conditions.

The present article starts by reviewing the experimental data available for both CH_4-CO_2 (Table 1) and CH_4-CO_2-H_2O (Table 2) systems at equilibrium conditions involving a CO_2-rich liquid phase. Then, the apparatus and approaches used to generate the new data are briefly described. In the third part of the paper, new experimental data will be presented and discussed.

Table 1. Experimental data for the CH_4-CO_2 binary system at vapour-liquid equilibrium (VLE), between 273.15 and 301 K.

Isotherm Studied (K)	Pressure Range (MPa)	Number of Data Points (x_{CH_4}, y_{CH_4})	Reference
273.15 283.15	5.20–8.08 6.12–8.08	(3, 4) (3, 3)	[13]
273.15 288.15	4.15–8.41 5.38–8.04	(3, 9) (5, 7)	[14]
288.50 293.40	5.12–8.15 5.73–7.98	(10, 10) (13, 13)	[15]
301.00	6.86–7.70	(6, 6) + Critical point	[16]
274.15 277.15 283.15 288.15 290.15	3.64–8.33 3.94–8.20 4.60–8.08 5.17–7.63 5.44–7.82	(9, 0) (11, 0) (4, 0) (4, 0) (6, 0)	This work

Table 2. Available experimental data for the CO_2-H_2O binary and CH_4-CO_2-H_2O ternary mixtures involving a CO_2-rich liquid phase.

System	Phases	*T* (K) *p* (MPa)	CH_4 Composition	Data	Reference
CO_2-H_2O	H-L_{H_2O}-L_{CO_2}-V Point in *p*-*T* space	283.19 (±0.46) 4.49 (±0.20)	-	9	[17–25]
	H-L_{H_2O}-L_{CO_2} Line in *p*-*T* space	282.92–294.00 4.5–494	-	61	[23–31]
CH_4-CO_2-H_2O	H-L_{H_2O}-L_{CO_2}-V Line in *p*-*T* space	283.86–285.56 4.930–6.720	0.0517–0.1750 (y_{CH_4}, vapor phase)	3	[17]
		283.86–285.76 4.930–7.251	0.0596–0.2026 (y_{CH_4}, vapor phase)	4	[18]
		283.51–287.04 4.74–8.37	0.05–0.22 ($z^*_{CH_4}$, gas load)	18	[19]
		283.90–286.19 4.925–7.62	-	5	[32]
		284.15 5.81	0.059 ($z^*_{CH_4}$, gas load)	1	[33]
	H-L_{H_2O}-L_{CO_2} Surface in *p*-*T* space	285.75–286.95 12.25–19.97	0.059 ($z^*_{CH_4}$, gas load)	2	[33]
		285.11–288.39 7.17–27.71	0.100–0.154 ($z^*_{CH_4}$, gas load)	7	This work

An important requirement for the development of CH_4 hydrate production coupled with CO_2-sequestration is the knowledge of the contents of H_2O and CH_4 lost in the liquid CO_2. Currently, a lack of CH_4 solubility data for the liquid CO_2 phase [34] hinders thermodynamic models to accurately evaluate the amount of CH_4 that is lost in the liquid CO_2 phase for such a production scheme. Few works have measured the phase properties of such mixtures at high pressures and temperatures

ranging between 273.15 and 301 K (Table 1). Clearly, more measurements are needed in order to develop accurate thermodynamic models to quantitatively assess the CH_4-to-CO_2 hydrate conversion process.

Phase equilibria of the CH_4-CO_2 binary mixture have previously been investigated to determine its phase envelopes and phase compositions as a function of temperature and pressure [34,35]. This binary mixture exhibits a diagram of Type I in the classification of van Konynenburg [32,36]. Thus, in the pressure-composition space, the vapor-liquid equilibrium (VLE) envelopes are characterized by critical points located along a continuous line linking the critical points of CH_4 (190.55 K; 4.60 MPa) and CO_2 (304.21 K; 7.38 MPa) [37]. However, few data points are available for the CH_4-CO_2 VLE in the temperature range of 273.15 and 301 K (Table 1). This range is located between the freezing point of H_2O and the critical temperature of CO_2, and also includes the typical marine conditions favorable for the formation of gas hydrates.

Arai et al. [14] performed the VLE in a glass capillary cell. The pressure was then increased while keeping the temperature constant, and the resulting volume change of the mixture was measured with a cathetometer. The bubble point was determined by analyzing the pressure change with respect to the molar volume due to the vanishing of the vapor phase. Kaminishi et al. [13,38] investigated the VLE inside a high-pressure-stirred cell, and they were able to sample both phases. Xu et al. [15,39] used a similar method as the present work, with a gas chromatograph to analyze liquid and gas sampled from a high-pressure cell. Bian et al. [16] used a static method to analyze both phases and the critical pressure.

The CH_4-CO_2-H_2O ternary system has been studied under multiple phase equilibrium. Al Ghafri et al. [32] did a very interesting study of this mixture at VLE, vapor-liquid-liquid equilibrium (VLLE), liquid-liquid equilibrium (LLE), and hydrate-vapor-liquid-liquid equilibrium (HVLLE). Indeed, in the *p*–*T* diagram, the VLLE region delimited by the Quadruple curve, the upper-critical end point (UCEP) curve, and the CO_2 vaporization curve has been studied by Al Ghafri et al. [32], with composition measurements for all phases.

The CH_4-CO_2-H_2O ternary system is able to form a CO_2-rich liquid phase under relatively higher pressure, and this drastically changes the hydrate stability field in comparison with pure CO_2. However, experimental data at hydrate-liquid-liquid equilibrium (HLLE) conditions are scarce (see comprehensive summary in Table 2). Considering experimental data from all authors, the temperatures investigated are between 282.92 and 294 K, with pressures ranging from 4.5 to 494 MPa, and the initial load of CO_2 varying from 0.78 to 1 mole fraction. The data below 30 MPa are shown for the HVLLE and the HLLE in Figure 1, together with calculated dissociation curves of gas hydrate for pure CH_4 and pure CO_2 gas hydrate formers, and vapor pressure of pure CO_2 [40].

The occurrence of the CO_2-rich liquid phase is possible for such ternary systems with gas hydrates only for CH_4 mole fractions of 0-0.225 for the initial CH_4-CO_2 gas feed [19]. Thus, it is possible to have an upper-quadruple point (Q_2) where gas hydrate (H), liquid H_2O (L_{H_2O}), CO_2-rich liquid (L_{CO_2}), and vapor (V) phases coexist (HVLLE) [19]. However, for a given temperature, the CH_4-CO_2-H_2O system is able to form a CO_2-rich liquid phase under higher pressures than for pure CO_2. The quadruple points Q_2 for such mixtures are located at higher pressures, shifting the hydrate stability zone towards the high-pressure region accordingly. The Q_2 for a CH_4 molar fraction of 0.225 has been estimated by Bi et al. [19] to be at 287.9 K and 8.4 MPa. Thus, the Q_2 zone is accurately described by several authors [17–19,32] (Table 2) (Figure 1, "+" orange symbols).

For temperatures below Q_2, or a richer CH_4 mole fraction, the area is well described and several stability points of mixed gas hydrates with vapor and aqueous phase, the hydrate-vapor-liquid equilibrium (HVLE), monitoring have been published as reviewed by Kastanidis et al. [41]. The same is true for the gas hydrate stability in the presence of a pure CO_2-rich liquid phase (HLLE) (Table 2), whereas data for CH_4 admixtures in the CO_2-rich liquid phase exists only for 5.9 mol % CH_4 (Table 2) [33]. These authors measured gas hydrate dissociation points using an isochoric step-heating method, keeping the H_2O mole fraction between 0.53 and 0.57. The present article will also focus on the HLLE region with mixed CH_4-CO_2-hydrates.

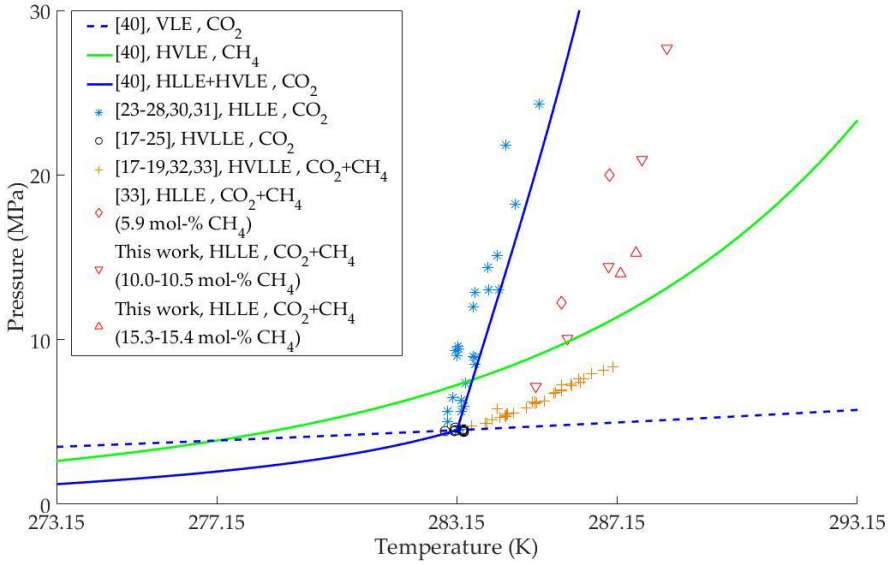

Figure 1. Available experimental data describing gas hydrate equilibria for the (CH_4)-CO_2-H_2O system in the presence of H-L_{H_2O}-L_{CO_2}-(V) phases below 30 MPa. HLLE: hydrate-liquid-liquid equilibrium; HVLE: hydrate-vapor-liquid equilibrium; HVLLE: hydrate-vapor-liquid-liquid equilibrium; VLE: vapor-liquid equilibrium.

2. Experiments

2.1. Experimental Apparatus

The phase equilibrium experiments were performed with the apparatus described by Ruffine et al. [42], which was modified to accommodate a high-pressure stirrer (minimaster, Premex Reactor AG, Lengnau, Switzerland) (Figure 2). It consists of a cylindrical 316Ti variable-volume high-pressure cell with a 17-4PH stainless steel moving piston (Hand-Operated Pressure Generator with optical cell, SITEC-Sieber Engineering AG, Maur, Switzerland). The cell can be operated at pressures up to 60 MPa, and temperatures ranging between 253 and 473 K. The volume of the cell varies from 20.8 ($\pm$0.6) to 65.4 ($\pm$0.3) mL. Both ends of the cell are closed by a sapphire window. At the top of the cell, a ROLSI^{TM} sampler (Rapid On-Line Sampler-Injector, Armines-CTP/MINES ParisTech, Fontainebleau, France) [43] was connected to a TCD-FID (Thermal Conductivity Detector-Flame Ionization Detector)-coupled GC-MS (Gas Chromatography-Mass Spectrometry) (7890A-5975C, Agilent, Santa Clara, CA, USA), allowing the withdrawal of an aliquot of a selected phase for compositional analysis. The GC-MS data were processed with the MSDChem software and the Chemstation integrator (Agilent, Santa Clara, CA, USA). To avoid condensation or partial vaporization of the sample, both the ROLSI^{TM} and the transfer line were heated up to 423 K with a thermal resistance controlled by a West 6100+ interface (ISE Inc., Cleveland, OH, USA). A high-pressure stirrer was connected at the bottom port of the cell to improve the mixing and shorten the time needed to achieve thermodynamic equilibrium. The stirrer speed, set by a 24 V/DC motor, could be varied between 200 and 1500 rpm. A high-pressure metering pump (Optos, Eldex Laboratories Inc., Napa, CA, USA) was used to inject liquids into the cell at pressures of up to 52.5 MPa with an adjustable flow rate of 0.1–10.0 mL min^{-1}. The thermal regulation was achieved using a compact cooling circulator (ministat 230, Huber Kältemaschinenbau AG, Offenburg, Germany) filled with a mixture of H_2O/EtOH (50/50 vol %).

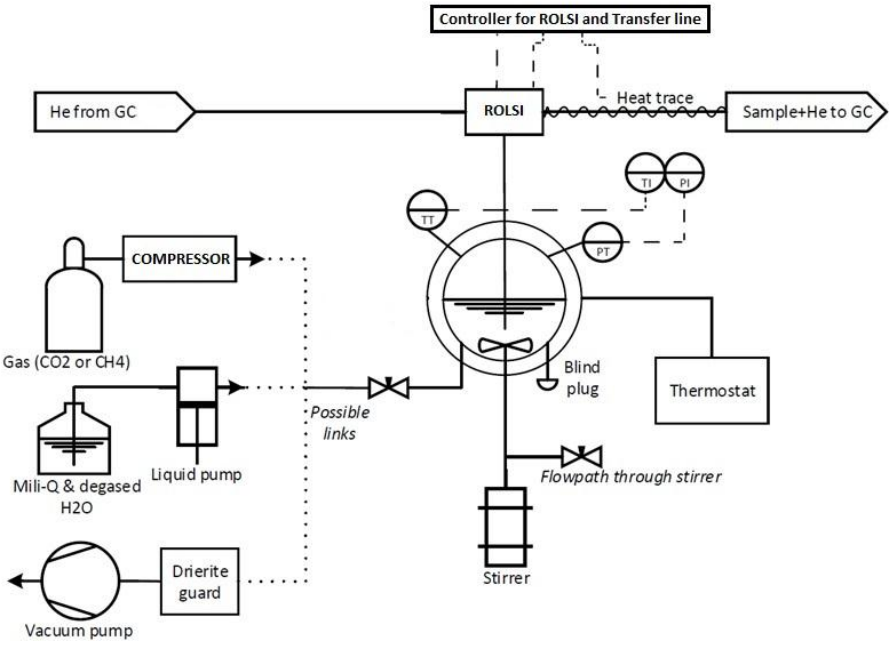

Figure 2. Sketch of the experimental set-up including the high-pressure cell, modified from Ruffine et al. [42].

2.2. Materials

All gases—pure components or gas mixtures—were supplied by L'Air Liquide. CH_4 and CO_2 had a claimed purity of 99.99 mol-%, while the standard mixture of CH_4-CO_2 had a certified composition of 10.04 (±0.20) mol-% of CH_4. For all experiments requiring H_2O, MilliQ-H_2O with a resistivity of 18.2 MΩ cm was degassed prior to the injection.

2.3. Experimental Procedure

For VLE, CO_2 was injected first at the desired temperature, followed by the injection of CH_4 into the cell until reaching the desired final pressure. Equilibrium was reached quickly by using the stirrer. The composition of the liquid phase was analyzed with the GC.

For gas hydrate experiments, the temperature of the cell was set to 288.15 K and its volume to the maximum. A custom-made CH_4-CO_2 gas mixture, obtained from pure CH_4 and CO_2, was used for Mixtures 1, 2, 3, 6, 7, and the standard mixture from L'Air Liquide for Mixtures 4 and 5. The composition of the custom-made mixture was determined by GC. The cell volume was then reduced to form a liquid phase by pressure increase. H_2O was injected afterwards, and the temperature was reduced to 276.85 K to allow the formation of gas hydrates. An isochoric stepwise heating procedure [44] with temperature increments of 0.5 K every 5 h was applied to determine the hydrate dissociation conditions. The composition of the CO_2-rich liquid phase was measured by discrete sampling during gas hydrate formation and dissociation.

3. Results and Discussion

3.1. CH_4-CO_2 Binary System

Data at 288.15 and 283.15 K were used to validate the experimental procedure for the VLE study by comparison with those from Arai et al. [14] and Kaminishi et al. [13] (Table 3). Our data agree well with those of both research groups. For the isotherm at 283.15 K, our composition data at 8.08 MPa has a relative deviation from the one of Kaminishi et al. [13] by 2.1 %. Finally, the vapor pressures of pure CO_2 for all isotherms were compared to the correlation from NIST [45,46] (Table 3).

Five isotherms were built from experiments performed at a temperature range of 274.15 to 290.15 K (Table 4, Figure 3) to complete the current database (Table 1). When comparing these data points to modelled isotherms [40] based on the established algorithm of Duan [35] which uses the Soave–Redlich–Kwong (SRK) equation of state (EoS), a good fit is obtained. This binary system has also been studied by Vitu et al. [34], using a group contribution approach and the Predictive PR78 EoS model including a temperature-dependent binary interaction parameter of 0.093–0.112.

Table 3. Relative deviation (RD) of solubility data (mole fractions) and vapor pressures (of pure CO_2 with $x_{CH_4} = 0$) between this work and literature values.

RD %	T (K)	p (MPa)	x_{CH_4}	Reference
−5.4 (x_{CH_4})	288.15	7.63 7.65	0.1097 0.1160	This work [14]
−2.1 (x_{CH_4})	283.15	8.08 8.08	0.1732 0.177	This work [13]
1.7 (p)	274.15	3.64 3.58	0 0	This work [45,46]
1.8 (p)	277.15	3.94 3.87	0 0	This work [45,46]
2.2 (p)	283.15	4.60 4.50	0 0	This work [45,46]
1.6 (p)	288.15	5.17 5.09	0 0	This work [45,46]
1.9 (p)	290.15	5.44 5.34	0 0	This work [45,46]

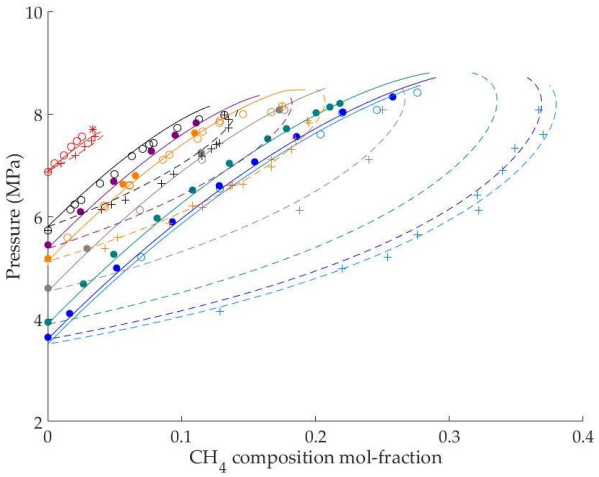

Figure 3. Liquid and vapor phase compositions of the CH_4-CO_2 mixture between 273.15 and 301 K along eight isotherms: T = 273.15 K (cyan); T = 274.15 K (blue); T = 277.15 K (green); T = 283.15 K (grey); T = 288.15 K (288.5 K for Xu et al. [15] data) (orange); T = 290.15 K (purple); T = 293.4 K (black); T = 301 K (red). Experimental bubble points x_{CH_4} from this work (filled dot), experimental bubble points x_{CH_4} from other authors (empty dot), experimental dew points y_{CH_4} from other authors (cross), critical point (star) [13–16]. Modelling of the bubble lines (solid-lines) and the dew lines (dotted-lines) is based on the SRK-EoS.

In this work, a thermodynamic model was developed based on the SRK-EoS and applied to the system CH_4-CO_2. A temperature-dependent binary interaction parameter $k_{ij(CH_4\text{-}CO_2)} = 1.32 \times 10^{-3} \times T - 0.251$ was optimized over the temperature interval corresponding to the experimental bubble

points between 274.15 and 290.15 K. A good agreement was also obtained for measurements outside of this temperature range (i.e., for the dew points and at 273.15, 293.4, and 301 K; Figure 3), demonstrating the predictive capability of the EoS. However, the present model does not reproduce the behavior of the system near the critical point with satisfactory accuracy. Thus, provided that the conditions of interest are not close to the critical point, a simple model based on a cubic EoS allows for a good description of the CH_4-CO_2 mixture at VLE at the temperature and pressure ranges encountered in most of the marine environment of interest for our study (i.e., CO_2-rich seeps and gas hydrate deposits on continental margins). This is convenient to implement, for example, into gas hydrate reservoir models where a more sophisticated EoS would increase computational time too much.

Table 4. Experimental measurements of bubble points (molar fraction of CH_4 in the liquid phase) on the CH_4-CO_2 binary system.

T (K)	p (MPa)	x_{CH_4}	T (K)	p (MPa)	x_{CH_4}
274.15	3.64	0	277.15	8.02	0.2005
274.15	4.11	0.0166	277.15	8.13	0.2107
274.15	4.99	0.0518	277.15	8.20	0.2185
274.15	5.90	0.0929	283.15	4.60	0
274.15	6.60	0.1284	283.15	5.37	0.0293
274.15	7.06	0.1545	283.15	7.24	0.1145
274.15	7.56	0.186	283.15	8.08	0.1732
274.15	8.04	0.2206	288.15	5.17	0
274.15	8.33	0.2577	288.15	6.62	0.0566
277.15	3.94	0	288.15	6.80	0.0654
277.15	4.69	0.0266	288.15	7.63	0.1097
277.15	5.26	0.0495	290.15	5.44	0
277.15	5.97	0.0817	290.15	6.09	0.0243
277.15	6.51	0.1083	290.15	6.69	0.0496
277.15	7.04	0.1358	290.15	7.27	0.0772
277.15	7.51	0.1643	290.15	7.59	0.0951
277.15	7.71	0.1786	290.15	7.82	0.1107

3.2. CH_4-CO_2-H_2O Ternary System

Seven gas hydrate dissociation points delimiting the HLLE were measured for CH_4 mole fractions of 0.1–0.105 and 0.153–0.154 of the initial gas mixture (Table 5). The experimental data were compared with calculations of the CSMGem program [47]. The program systematically underestimated the gas hydrate dissociation pressure, with absolute deviations up to 7 MPa compared to our experimental data (Table 5). The p–T curve of gas hydrate dissociation of pure CO_2 is strongly dependent on the temperature, showing a very steep slope. Likewise, the CH_4-CO_2 mixed gas hydrate dissociation appears to be strongly dependent on the temperature when no vapor phase is present (Figure 1).

Table 5. Experimental data of H-L_{H_2O}-L_{CO_2} equilibria (HLLE) for the CH_4-CO_2-H_2O ternary system. Values inside brackets are CSMGem [47] model values applied on the system.

Title		Mix. 1	Mix. 2	Mix. 3	Mix. 4	Mix. 5	Mix. 6	Mix. 7
Composition Mole fraction	$z^*_{CH_4}$	0.105	0.105	0.105	0.100	0.100	0.153	0.154
	z_{CH_4}	0.031	0.043	0.038	0.029	0.052	0.103	0.090
	z_{CO_2}	0.266	0.369	0.328	0.263	0.467	0.572	0.492
	z_{H_2O}	0.703	0.588	0.634	0.708	0.481	0.325	0.418
	$x^*_{CH_4}$ without gas hydrate	0.102 (0.088)	0.110 (0.108)	0.111 (0.108)	0.106 (0.105)	0.106 (0.102)	0.154 (0.154)	0.155 (0.157)
	$x^*_{CH_4}$ with gas hydrate	0.095 (0.060)	0.102 (0.072)	0.106 (0.063)	0.092 (0.097)	0.089 (0.073)	0.152 (0.138)	0.149 (0.133)
Gas hydrate dissociation	T (K)	285.11	285.90	286.93	287.77	288.39	287.24	287.61
	p (MPa)	7.17 (6.33)	10.07 (7.52)	14.45 (11.73)	20.94 (16.54)	27.71 (20.87)	13.99 (10.72)	15.25 (12.08)

The CH_4-to-CO_2 concentration ratio (i.e., without considering H_2O composition, $x^*_{CH_4}$) in the CO_2-rich liquid phase decreased when gas hydrate was formed. In order to understand if this change is caused by hydrate formation or simply a *p–T* -effect, the CSMGem program [47] is here employed on the data (Table 5). Considering a case study with Mixture 2 at 288.15 K and 10 MPa, CSMGem predicts an aqueous and a CO_2-rich liquid phase, as is visually observed in our experiments (Table 5). CSMGem computes that CH_4 amounts to only 2% of the dissolved gases in the aqueous phase; i.e., $x^*_{CH_4}/(x^*_{CH_4} + x^*_{CO_2})$. Indeed, the CO_2 is more soluble than CH_4 in liquid H_2O, and hence CH_4 is enriched in the CO_2-rich liquid phase when H_2O is pumped into the CH_4-CO_2 mixture (Table 5, $x^*_{CH_4}$ without gas hydrate). When the temperature is decreased from 288.15 to 276.85 K, mixed gas hydrates containing a CH_4/CO_2 ratio of 21/79 should form (CSMGem), thereby reducing the CH_4-to-CO_2 ratio in the CO_2-rich liquid phase, as it was observed in the experiments.

The formation of gas hydrate was visually observed, relatively rapidly after the start of the stirring. Gas hydrates accumulated rapidly in the cell, and the stirrer was then switched off to prevent any damage (Figure 4). It was visually observed that the gas hydrate formed first at the H_2O phase interface and then grew in the H_2O phase before spreading across the entire surface of the sapphire window, blocking the view (Figure 4).

The time of incipient gas hydrate formation and the stirring conditions are summarized in Table 6 with no evident correlation between time of gas hydrate formation start and initial setup (composition, pressure, stirring speed).

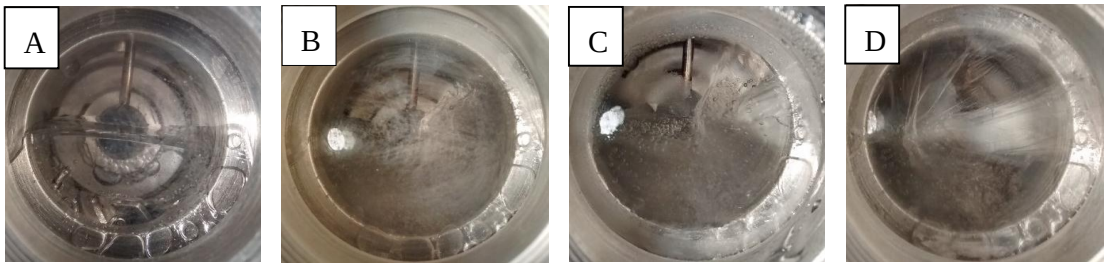

Figure 4. Photos showing different steps during gas hydrate formation and dissociation with Mixture 2. From left to right: (**A**) after H_2O injection (L_{H_2O}-L_{CO_2}); (**B**) just after incipient formation start (H-L_{H_2O}-L_{CO_2}); (**C**) ca. 40 min after formation start (H-L_{H_2O}-L_{CO_2}); (**D**) ca. 170 min after formation start (H-L_{H_2O}-L_{CO_2}).

Table 6. Incipient gas hydrate time of formation on the CH_4-CO_2-H_2O ternary system.

Title	Mix. 1	Mix. 2	Mix. 3	Mix. 4	Mix. 5	Mix. 6	Mix. 7
Stirrer rotation speed (rpm)	1000	1000	1000	100	100	700	700
Time of incipient formation (min)	18	14	33	18	10	10	56

4. Conclusions

Mixtures of CH_4-CO_2 and CH_4-CO_2-H_2O involving a CO_2-rich liquid phase are investigated under *p–T* conditions typical for marine environments, such as CO_2-rich seeps of volcanic origin and gas hydrate deposits suitable for gas production via CO_2 injection.

VLE data were measured and modelled with a simple Soave–Redlich–Kwong EoS for the CH_4-CO_2 system, at conditions between the freezing point of H_2O and the critical point of CO_2. This model enables, for example, the accurate prediction of how much CH_4 is retained in the CO_2-rich liquid phase. Subsequently, a set of data on gas hydrate dissociation was measured to evaluate the phase behavior of CH_4-CO_2 hydrate containing a CO_2-rich liquid phase without any vapor phase. The measurements collected in this newly explored phase region (CH_4-CO_2-H_2O HLLE) indicate that the added CH_4 increases the stability of the resulting gas hydrates, which is the opposite trend

compared to the region where a vapor phase is stable. Moreover, the formation of gas hydrates in this system consequently reduces the CH_4 in the coexisting CO_2-rich liquid phase.

For a CH_4 production scenario under the investigated *p–T* conditions, this study indicates that mixed CH_4-CO_2 hydrates are more stable than pure CO_2 hydrates, thus allowing the storage of CO_2 in mixed gas hydrates under an extended temperature range for a given pressure. In addition, a more accurate model for calculating the CH_4 content in the dense CO_2 liquid phase is under development, which will improve the mass balancing of reservoir simulations of CH_4 hydrate production via CO_2 injection and also improve our understanding of the phase behavior of natural liquid CO_2 seeps, where CH_4 is a common admixture.

The CH_4-CO_2-H_2O system still needs to be further investigated in the phase region presented here, particularly in the HLLE domain at the lower and upper end of CH_4 concentrations allowing for a CO_2-rich liquid phase. Indeed, already small additions of CH_4 drastically affect the gas hydrate stability pressure, whereas high concentrations would provide more insights into the border of the HLLE region.

Acknowledgments: This work was supported by the SUGAR project, funded by the German Ministry of Research (Grant No. 03G0856A), and the 'Hydrate as Geohazards' project from the Unité des Géosciences Marines (IFREMER).

Author Contributions: Ludovic Nicolas Legoix and Livio Ruffine conceived and designed the experiments; Ludovic Nicolas Legoix, Livio Ruffine and Jean-Pierre Donval performed the experiments; Ludovic Nicolas Legoix analyzed the data; Ludovic Nicolas Legoix, Matthias Haeckel and Livio Ruffine wrote the paper.

Conflicts of Interest: The authors declare no conflict of interest.

Abbreviations

	Symbol	Unit
CO_2-rich liquid phase composition of molecule *i*	x_i	mole fraction
CO_2-rich liquid phase composition of molecule *i* without H_2O	x^*_i	mole fraction
Vapour phase composition of molecule *i*	y_i	mole fraction
Global composition of molecule *i* in the system	z_i	mole fraction
Global composition of molecule *i* in the system without H_2O	z^*_i	mole fraction

References

1. Lewicki, J.L.; Birkholzer, J.; Tsang, C.F. Natural and industrial analogues for leakage of CO_2 from storage reservoirs: Identification of features, events, and processes and lessons learned. *Environ. Geol.* **2007**, *52*, 457–467. [CrossRef]
2. Boiron, M.C.; Cathelineau, M.; Ruggieri, G.; Jeanningros, A.; Gianelli, G.; Banks, D.A. Active contact metamorphism and CO_2–CH_4 fluid production in the Larderello geothermal field (Italy) at depths between 2.3 and 4 km. *Chem. Geol.* **2007**, *237*, 303–328. [CrossRef]
3. Sakai, H.; Gamo, T.; Kim, E.S.; Tsutsumi, M.; Tanaka, T.; Ishibashi, J.; Wakita, H.; Yamano, M.; Oomori, T. Venting of carbon dioxide-rich fluid and hydrate formation in mid-Okinawa trough backarc basin. *Science* **1990**, *248*, 1093–1097. [CrossRef] [PubMed]
4. Inagaki, F.; Kuypers, M.M.; Tsunogai, U.; Ishibashi, J.I.; Nakamura, K.I.; Treude, T.; Ohkubo, S.; Nakaseama, M.; Gena, K.; Chiba, H.; et al. Microbial community in a sediment-hosted CO_2 lake of the southern Okinawa Trough hydrothermal system. *Proc. Natl. Acad. Sci. USA* **2006**, *103*, 14164–14169. [CrossRef] [PubMed]
5. Konno, U.; Tsunogai, U.; Nakagawa, F.; Nakaseama, M.; Ishibashi, J.I.; Nunoura, T.; Nakamura, K.I. Liquid CO_2 venting on the seafloor: Yonaguni Knoll IV hydrothermal system, Okinawa Trough. *Geophys. Res. lett.* **2006**, *33*. [CrossRef]
6. Lupton, J.; Butterfield, D.; Lilley, M.; Evans, L.; Nakamura, K.I.; Chadwick, W.; Resing, J.; Emblez, R.; Olson, E.; Proskurowski, G.; et al. Submarine venting of liquid carbon dioxide on a Mariana Arc volcano. *Geochem. Geophys.* **2006**, *7*. [CrossRef]

7. Ebinuma, T. Method for Dumping and Disposing of Carbon Dioxide Gas and Apparatus Therefor. U.S. Patent 5,261,490, 16 November 1993.
8. Nakano, S.; Yamamoto, K.; Ohgaki, K. Natural gas exploitation by carbon dioxide from gas hydrate fields—High-pressure phase equilibrium for an ethane hydrate system. *Proc. Inst. Mech. Eng. A J. Power Energy* **1998**, *212*, 159–163. [CrossRef]
9. Ota, M.; Morohashi, K.; Abe, Y.; Watanabe, M.; Smith, R.L., Jr.; Inomata, H. Replacement of CH_4 in the hydrate by use of liquid CO_2. *Energy Convers. Manag.* **2005**, *46*, 1680–1691. [CrossRef]
10. Schicks, J.M.; Spangenberg, E.; Giese, R.; Steinhauer, B.; Klump, J.; Luzi, M. New approaches for the production of hydrocarbons from hydrate bearing sediments. *Energies* **2011**, *4*, 151–172. [CrossRef]
11. Deusner, C.; Bigalke, N.; Kossel, E.; Haeckel, M. Methane production from gas hydrate deposits through injection of supercritical CO_2. *Energies* **2012**, *5*, 2112–2140. [CrossRef]
12. Boswell, R.; Schoderbek, D.; Collett, T.S.; Ohtsuki, S.; White, M.; Anderson, B.J. The Ignik Sikumi Field Experiment, Alaska North Slope: Design, Operations, and Implications for CO_2-CH_4 Exchange in Gas Hydrate Reservoirs. *Energy Fuels* **2016**, *31*, 140–153. [CrossRef]
13. Kaminishi, G.I.; Arai, Y.; Saito, S.; Maeda, S. Vapor-liquid equilibria for binary and ternary systems containing carbon dioxide. *J. Chem. Eng. Jpn.* **1968**, *1*, 109–116. [CrossRef]
14. Arai, Y.; Kaminishi, G.I.; Saito, S. The experimental determination of the PVTX relations for the carbon dioxide-nitrogen and the carbon dioxide-methane systems. *J. Chem. Eng. Jpn.* **1971**, *4*, 113–122. [CrossRef]
15. Xu, N.; Dong, J.; Wang, Y.; Shi, J. High pressure vapor liquid equilibria at 293 K for systems containing nitrogen, methane and carbon dioxide. *Fluid Phase Equilib.* **1992**, *81*, 175–186. [CrossRef]
16. Bian, B.; Wang, Y.; Shi, J.; Zhao, E.; Lu, B.C.Y. Simultaneous determination of vapor-liquid equilibrium and molar volumes for coexisting phases up to the critical temperature with a static method. *Fluid Phase Equilib.* **1993**, *90*, 177–187. [CrossRef]
17. Seo, Y.T.; Kang, S.P.; Lee, H.; Lee, C.S.; Sung, W.M. Hydrate phase equilibria for gas mixtures containing carbon dioxide: A proof-of-concept to carbon dioxide recovery from multicomponent gas stream. *Korean J. Chem. Eng.* **2000**, *17*, 659–667. [CrossRef]
18. Seo, Y.T.; Lee, H. Multiple-phase hydrate equilibria of the ternary carbon dioxide, methane, and water mixtures. *J. Phys. Chem. B* **2001**, *105*, 10084–10090. [CrossRef]
19. Bi, Y.; Yang, T.; Guo, K. Determination of the upper-quadruple-phase equilibrium region for carbon dioxide and methane mixed gas hydrates. *J. Pet. Sci. Eng.* **2013**, *101*, 62–67. [CrossRef]
20. Unruh, C.H.; Katz, D.L. Gas hydrates of carbon dioxide-methane mixtures. *J. Petrol. Technol.* **1949**, *1*, 83–86. [CrossRef]
21. Robinson, D.B.; Metha, B.R. Hydrates in the propane carbon dioxide-water system. *J. Can. Petrol. Technol.* **1971**, *10*. [CrossRef]
22. Yoon, J.H.; Lee, H. Clathrate phase equilibria for the water-phenol-carbon dioxide system. *AIChE J.* **1997**, *43*, 1884–1893. [CrossRef]
23. Fan, S.S.; Guo, T.M. Hydrate formation of CO_2-rich binary and quaternary gas mixtures in aqueous sodium chloride solutions. *J. Chem. Eng. Data* **1999**, *44*, 829–832. [CrossRef]
24. Mooijer-Van Den Heuvel, M.M.; Witteman, R.; Peters, C.J. Phase behaviour of gas hydrates of carbon dioxide in the presence of tetrahydropyran, cyclobutanone, cyclohexane and methylcyclohexane. *Fluid Phase Equilib.* **2001**, *182*, 97–110. [CrossRef]
25. Ruffine, L.; Trusler, J.P.M. Phase behaviour of mixed-gas hydrate systems containing carbon dioxide. *J. Chem. Thermodyn.* **2010**, *42*, 605–611. [CrossRef]
26. Takenouchi, S.; Kennedy, G.C. The binary system H_2O-CO_2 at high temperatures and pressures. *Am. J. Sci.* **1964**, *262*, 1055–1074. [CrossRef]
27. Ng, H.J.; Robinson, D.B. Hydrate formation in systems containing methane, ethane, propane, carbon dioxide or hydrogen sulfide in the presence of methanol. *Fluid Phase Equilib.* **1985**, *21*, 145–155. [CrossRef]
28. Ohgaki, K.; Makihara, Y.; Takano, K. Formation of CO_2 hydrate in pure and sea waters. *J. Chem. Eng. Jpn.* **1993**, *26*, 558–564. [CrossRef]
29. Nakano, S.; Moritoki, M.; Ohgaki, K. High-pressure phase equilibrium and Raman microprobe spectroscopic studies on the CO_2 hydrate system. *J. Chem. Eng. Data* **1998**, *43*, 807–810. [CrossRef]

30. Chapoy, A.; Burgass, R.; Tohidi, B.; Austell, J.M.; Eickhoff, C. Effect of common impurities on the phase behavior of carbon-dioxide-rich systems: Minimizing the risk of hydrate formation and two-phase flow. *SPE J.* **2011**, *16*, 921–930. [CrossRef]
31. Alsiyabi, I.; Chapoy, A.; Tohidi, B. Effect of common impurities on the hydrate stability of carbon dioxide systems. In Proceedings of the 8th International Conference on Gas Hydrates (ICGH8-2014), Beijing, China, 28 July–1 August 2014.
32. Al Ghafri, S.Z.; Forte, E.; Maitland, G.C.; Rodriguez-Henríquez, J.J.; Trusler, J.M. Experimental and modeling study of the phase behavior of (methane + CO_2 + water) mixtures. *J. Phys. Chem. B* **2014**, *118*, 14461–14478. [CrossRef] [PubMed]
33. Chapoy, A.; Burgass, R.; Tohidi, B.; Alsiyabi, I. Hydrate and phase behavior modeling in CO_2-Rich pipelines. *J. Chem. Eng. Data* **2014**, *60*, 447–453. [CrossRef]
34. Vitu, S.; Jaubert, J.N.; Pauly, J.; Daridon, J.L.; Barth, D. Bubble and dew points of carbon dioxide + a five-component synthetic mixture: Experimental data and modeling with the PPR78 model. *J. Chem. Eng. Data* **2008**, *52*, 1851–1855. [CrossRef]
35. Duan, Z.; Hu, J. A new cubic equation of state and its applications to the modeling of vapor-liquid equilibria and volumetric properties of natural fluids. *Geochim. Cosmochim. Acta* **2004**, *68*, 2997–3009. [CrossRef]
36. Van Konynenburg, P.H.; Scott, R.L. Critical lines and phase equilibria in binary van der Waals mixtures. *Philos. Trans. R. Soc. A* **1980**, *298*, 495–540. [CrossRef]
37. Poling, B.E.; Prausnitz, J.M.; O'Connell, J.P. *The Properties of Gases and Liquids*; McGraw-Hill: New York, NY, USA, 2001; Volume 5.
38. Kaminishi, G.; Toriumi, T. Gas-liquid equilibrium under high pressures VI. Vapor-liquid phase equilibrium in the CO_2-H_2, CO_2-N_2, and CO_2-O_2 systems. *Kogyo Kagaku Zasshi* **1966**, *69*, 175–178. [CrossRef]
39. Xu, N.; Yao, J.; Wang, Y.; Shi, J.; Lu, B.C.Y. Vapor-liquid equilibria of five binary systems containing R-22. *Fluid Phase Equilib.* **1991**, *69*, 261–270. [CrossRef]
40. Kossel, E.; Bigalke, N.K.; Pinero, E.; Haeckel, M. *The SUGAR Toolbox: A Library of Numerical Algorithms and Data for Modelling of Gas Hydrate Systems and Marine Environments*; PANGAEA: Bremen, Germany, 2013.
41. Kastanidis, P.; Romanos, G.E.; Stubos, A.K.; Economou, I.G.; Tsimpanogiannis, I.N. Two- and three-phase equilibrium experimental measurements for the ternary CH_4 + CO_2 + H_2O mixture. *Fluid Phase Equilib.* **2017**, *451*, 96–105. [CrossRef]
42. Ruffine, L.; Donval, J.P.; Charlou, J.L.; Cremière, A.; Zehnder, B.H. Experimental study of gas hydrate formation and destabilisation using a novel high-pressure apparatus. *Mar. Pet. Geol.* **2010**, *27*, 1157–1165. [CrossRef]
43. Guilbot, P.; Valtz, A.; Legendre, H.; Richon, D. Rapid on-line sampler-injector: A reliable tool for HT-HP sampling and on-line GC analysis. *Analusis* **2000**, *28*, 426–431. [CrossRef]
44. Tohidi, B.; Burgass, R.W.; Danesh, A.; Østergaard, K.K.; Todd, A.C. Improving the accuracy of gas hydrate dissociation point measurements. *Ann. N. Y. Acad. Sci.* **2000**, *912*, 924–931. [CrossRef]
45. NIST Chemistry WebBook, SRD 69. Available online: Webbook.nist.gov/chemistry/fluid (accessed on 10 September 2017).
46. Span, R.; Wagner, W. A new equation of state for carbon dioxide covering the fluid region from the triple-point temperature to 1100 K at pressures up to 800 MPa. *J. Phys. Chem. Ref. Data* **1996**, *25*, 1509–1596. [CrossRef]
47. Sloan, E.D., Jr.; Koh, C. *Clathrate Hydrates of Natural Gases*; CRC Press: Boca Raton, FL, USA, 2007.